Advances in Applied Mathematics and Mechanics
Adv. Appl. Math. Mech., Vol. **9**, No. 4, pp. 964-989

DOI: 10.4208/aamm.2016.m1463
August 2017

# Structure-Preserving Wavelet Algorithms for the Nonlinear Dirac Model

Xu Qian[1,2], Hao Fu[1] and Songhe Song[1,3,*]

[1] *Department of Mathematics and Systems Science, National University of Defense Technology, Changsha, Hunan 410072, China*
[2] *Academy of Ocean Science and Engineering, National University of Defense Technology, Changsha, Hunan 410073, China*
[3] *State Key Laboratory of High Performance Computing, National University of Defense Technology, Changsha, Hunan 410073, China*

Received 23 February 2016; Accepted (in revised version) 8 September 2016

**Abstract.** The nonlinear Dirac equation is an important model in quantum physics with a set of conservation laws and a multi-symplectic formulation. In this paper, we propose energy-preserving and multi-symplectic wavelet algorithms for this model. Meanwhile, we evidently improve the efficiency of these algorithms in computations via splitting technique and explicit strategy. Numerical experiments are conducted during long-term simulations to show the excellent performances of the proposed algorithms and verify our theoretical analysis.

**AMS subject classifications**: 35Q41, 65D30, 65Z0

**Key words**: Structure-preserving, wavelet collocation, conservation laws, nonlinear Dirac equation.

## 1 Introduction

In this paper, we consider the nonlinear Dirac (NLD) model

$$\begin{cases} \Psi_t = A\Psi_x + \mathrm{i}f(|\Psi_1|^2 - |\Psi_2|^2)B\Psi, \\ \Psi_1(x,0) = \phi_1(x), \quad \Psi_2(x,0) = \phi_2(x), \end{cases} \tag{1.1}$$

where $\Psi = (\Psi_1, \Psi_2)^{\mathrm{T}}$ is a spinorial wave function of a particle with the spin-$\frac{1}{2}$; $\Psi_1$ and $\Psi_2$ are complex functions describing the up and down states of the spin-$\frac{1}{2}$ particle, respectively; $\mathrm{i} = \sqrt{-1}$ is the imaginary unit, $f(s)$ is a real function of a real variable $s$, $A$ and $B$

*Corresponding author.
*Email:* shsong@nudt.edu.cn (S. H. Song)

 ©2017 Global Science Press

https://doi.org/10.4208/aamm.2016.m1463 Published online by Cambridge University Press

are matrices

$$A=\begin{pmatrix} 0 & -1 \\ -1 & 0 \end{pmatrix}, \quad B=\begin{pmatrix} -1 & 0 \\ 0 & 1 \end{pmatrix}.$$

The Dirac equation, formulated by the British physicist Paul Dirac in 1928, has been playing a fundamental role in various areas of modern physics, especially in description of interacting particles and fields.

In this paper, the charge $\mathcal{Q}$, the energy $\mathcal{E}$ and the linear momentum $\mathcal{M}$ are defined by

$$\begin{aligned}
\mathcal{Q}(\Psi)(t)&=\int_{\mathbf{R}}(|\Psi_1(x,t)|^2+|\Psi_2(x,t)|^2)dx,\\
\mathcal{E}(\Psi)(t)&=\int_{\mathbf{R}}\left[\Im\left(\overline{\Psi}_1\frac{\partial}{\partial x}\Psi_2+\overline{\Psi}_2\frac{\partial}{\partial x}\Psi_1\right)+\widetilde{f}(|\Psi_1|^2-|\Psi_2|^2)\right]dx,\\
\mathcal{M}(\Psi)(t)&=\int_{\mathbf{R}}\Im\left(\overline{\Psi}_1\frac{\partial}{\partial x}\Psi_1+\overline{\Psi}_2\frac{\partial}{\partial x}\Psi_2\right)dx,
\end{aligned}$$

where $\Im(\Psi)$ and $\overline{\Psi}$ stand for the imaginary part and the conjugate of the complex quantity $\Psi$, and $\widetilde{f}$ is a primitive function of $f$.

The NLD equation (1.1) admits the following conservation laws [1]:

**Proposition 1.1.** If the solution $\Psi$ satisfies

$$\lim_{|x|\to+\infty}|\Psi(x,t)|=0 \quad \text{and} \quad \lim_{|x|\to+\infty}|\partial_x\Psi(x,t)|=0 \quad \text{uniformly for } t\in\mathbf{R},$$

then

$$\frac{d}{dt}\mathcal{Q}(t)=0, \quad \frac{d}{dt}\mathcal{E}(t)=0 \quad \text{and} \quad \frac{d}{dt}\mathcal{M}(t)=0.$$

This paper will focus on an important particular case [1] of the NLD equation (1.1)

$$\begin{cases}
\dfrac{\partial\Psi_1}{\partial t}+\dfrac{\partial\Psi_2}{\partial x}+\mathrm{i}m\Psi_1+2\mathrm{i}\lambda(|\Psi_2|^2-|\Psi_1|^2)\Psi_1=0,\\
\dfrac{\partial\Psi_2}{\partial t}+\dfrac{\partial\Psi_1}{\partial x}-\mathrm{i}m\Psi_2+2\mathrm{i}\lambda(|\Psi_1|^2-|\Psi_2|^2)\Psi_2=0,
\end{cases} \tag{1.2}$$

that is, $f(s)=m-2\lambda s$ in Eq. (1.1), where $m,\lambda\in\mathbf{R}$, $\lambda$ is the nonlinear parameter.

Given $\Psi_1=q_1+\mathrm{i}q_2$, $\Psi_2=q_3+\mathrm{i}q_4$ with $q_k$ $(k=1,2,3,4)$ being real functions, the NLD equation (1.2) is rewritten as a system of real-value equations

$$\begin{cases}
\dfrac{\partial}{\partial t}q_1+\dfrac{\partial}{\partial x}q_3-mq_2-2\lambda(q_3^2+q_4^2-q_1^2-q_2^2)q_2=0,\\
\dfrac{\partial}{\partial t}q_2+\dfrac{\partial}{\partial x}q_4+mq_1+2\lambda(q_3^2+q_4^2-q_1^2-q_2^2)q_1=0,\\
\dfrac{\partial}{\partial t}q_3+\dfrac{\partial}{\partial x}q_1+mq_4+2\lambda(q_3^2+q_4^2-q_1^2-q_2^2)q_4=0,\\
\dfrac{\partial}{\partial t}q_4+\dfrac{\partial}{\partial x}q_2-mq_3-2\lambda(q_3^2+q_4^2-q_1^2-q_2^2)q_3=0.
\end{cases} \tag{1.3}$$

https://doi.org/10.4208/aamm.2016.m1463 Published online by Cambridge University Press

Two kinds of analytical solutions have been derived for the NLD equation (1.1). One is the standing wave solution, the other is so-called "solitary wave solution". Nevertheless, analytical study of the NLD equation still faces several challenging obstacles, including stability analysis and well-posedness [2]. Since existing theoretical means for the NLD equation are not able to meet the harsh requirements in practical issues, numerical investigation turns to be more and more important approach to understanding physical behaviors of the model. Up to now, some reliable numerical methods have been constructed to solve the NLD equation (1.1), such as finite difference methods [3,4], finite volume method [5], spectral method [6], high-order accurate Runge–Kutta discontinuous Galerkin method [7, 8], and multi-symplectic Runge–Kutta (MSRK) method [1]. However, finite difference methods are almost of the second order accuracy and thus suffer rapid error growth with respect to time. Although spectral methods and discontinuous Galerkin methods can achieve high-order accuracy, they do not have general structure-preserving properties, especially, it is hard for them to conserve energy conservation law exactly, which would restrict them over long time computations. Symplectic and multi-symplectic methods can preserve the inner geometric structures of original problems. In fact, only with some specific conditions, symplectic-preserving algorithms can preserve energy and momentum conservation laws precisely. For example, Bridges and Reich [9] show that only if the Hamiltonian function $S(z)$ is quadratic in the state variable $z$, then the multi-symplectic scheme conserves energy and momentum conservation laws exactly. Especially for the MSRK method for the NLD equation in [1], although the charge can be conserved in the sense of the corresponding discretization, it can not preserve energy and momentum conservation laws exactly.

Our main proposal is to achieve a balance among effectiveness, high efficiency, and structure-preservation. In this paper, wavelet collocation method, which is based on the autocorrelation function of Daubechies scaling function, is used for spatial discretization. Since it makes the corresponding spatial differentiation matrix sparse and demands less computations, it has been used in many practical problems [10–13]. In detail, we first construct the energy-preserving wavelet (EPW) method, and then, the multi-symplectic wavelet (MSW) method as comparison, which is based on the multi-symplectic formulation of the NLD equation. We prove that both of the two methods can preserve charge exactly. Moreover, the EPW method can preserve energy conservation law under periodic boundary conditions, and the MSW method can hold the inner geometric structures of original problems. Both of the two properties would guarantee the effectiveness of proposed algorithms during long-time computations. However, the EPW and MSW methods are completely implicit. To reduce the computational cost, we take the splitting technique and symplectic Euler method into the multi-symplectic integrator. The splitting method was originally designed to improve the efficiency, accuracy and stability of numerical algorithms. Therefore, it is effective and efficient for solving coupled equations and complex nonlinear problems recently [14–18]. The advantage of the symplectic Euler method [20] lies in the fact that the generated full-discrete scheme is explicit or semi-explicit, which does not need to solve all of the nonlinear algebraic equations at

https://doi.org/10.4208/aamm.2016.m1463 Published online by Cambridge University Press

every time step.

The paper is organized as follows. In Section 2, we introduce the wavelet collocation method and some notations. In Section 3, the EPW method for the NLD equation is constructed and the corresponding conservative properties are investigated. In Section 4, based on the multi-symplectic formulation of the NLD equation, the multi-symplectic integrators, including the wavelet midpoint rule, splitting integrator and symplectic Euler method, are proposed. Numerical simulations are presented in Section 5, which show the effectiveness of the proposed algorithms. Finally, conclusions are made in Section 6.

## 2 Preliminaries and notations

In this paper, a wavelet collocation method, which is based on the autocorrelation function of Daubechies scaling function of order $M$, is used for spatial discretization. A Daubechies scaling function $g(x)$ with $M$ non-vanishing "filter coefficients" satisfies the scaling relation:

$$g(x)=\sum_{k=0}^{M-1} h_k g(2x-k), \tag{2.1}$$

with the support in $[0,M-1]$ and $(M/2-1)$ vanishing wavelet moments. Meanwhile, a multi-resolution analysis can be conducted on $L^2(R)$. Then, we define the autocorrelation function $\theta(x)$ of $g(x)$ as

$$\theta(x)=(g*g(-\cdot))(x)=\int g(x)g(t-x)dt. \tag{2.2}$$

Suppose that $V_J$ is the linear span of $\{\theta_{J,k}(x)=2^{J/2}\theta(2^Jx-k),\ k\in Z\}$, then it can be proved that $(V_J)_{J\in Z}$ forms a multi-resolution analysis where $\theta(x)$ plays the role of scaling function.

In virtue of (2.1), we deduce that

$$\theta(x)=\theta(2x)+\frac{1}{2}\sum_{l=1}^{M/2} c_{2l-1}(\theta(2x-2l+1)+\theta(2x-2l-1)). \tag{2.3}$$

It is easy to compute the function $\theta(x)$ and its derivatives in terms of the values at the integer points by solving an eigenvalue problem which is derived from the scaling relation (2.3).

Consider the periodic boundary condition $u(a,t)=u(b,t)$, where $a$ and $b$ are integers. For a fixed scale $J=constant$, we define an interpolation operator on $V_J$ (with the space step being $h=2^{-J}$) as

$$I_Ju(x)=2^{-\frac{J}{2}}\sum_k u(2^{-J}k)\theta_{J,k}(x)=\sum_k u(2^{-J}k)\theta(2^Jx-k). \tag{2.4}$$

https://doi.org/10.4208/aamm.2016.m1463 Published online by Cambridge University Press

Furthermore, if we differentiate (2.4) for $k$-times at collocation points, one has

$$\frac{\partial^k u_J(x_m,t)}{\partial x^k}=\sum_{n=a\cdot 2^J}^{b\cdot 2^J-1}u_J(x_n)\frac{d^k\theta(2^Jx_m-n)}{dx^k}=(B_kU_J)_m, \tag{2.5}$$

where $B_k$ is a $N\times N$ matrix with elements

$$(B_k)_{m,n}=\frac{d^k\theta(2^Jx_m-n)}{dx^k}=2^{kJ}\theta^{(k)}(m-n),\quad N=(b-a)\cdot 2^J,$$

is the grid number, and $U_J=(u(x_{a\cdot 2^J}),u(x_{a\cdot 2^J+1}),\cdots,u(x_{b\cdot 2^J-1}))$. Especially, $B_k$ can be expressed as

$$(B_k)_{m,n}=\begin{cases}2^{kJ}\theta^{(k)}(m-n), & m-(M-1)\le n\le m+(M-1),\\ 2^{kJ}\theta^{(k)}(-i), & m-n=N-i,1\le i\le M-1,\\ 2^{kJ}\theta^{(k)}(i), & n-m=N-i,1\le i\le M-1,\\ 0, & \text{otherwise.}\end{cases} \tag{2.6}$$

There is no analytical expression for $\theta^{(k)}(x)$ $(k=0,1,2,\cdots)$, but we can get the numerical values of the function $\theta^{(k)}(x)$ at integer point $x=i$ $(i=0,\pm1,\cdots,\pm(M-1))$. From the properties of $B_k$, we can notice that $B_{2k}$ is symmetric and $B_{2k+1}$ is skew-symmetric. For the detail, one can see [10,11] and references therein.

As usual, the spatial-temporal domain $[a,b]\times[0,T]$ is divided by

$$x_l=a+l\Delta x,\quad t^n=n\tau,$$

where $\Delta x=2^{-J}$ and $\tau$ are mesh sizes in the $x$ and $t$ directions, respectively. The approximation of $u(x,t)$ at the node $(u_l,t^n)$ is denoted by $u_l^n$. We present the notation for norm

$$\|u^n\|=\left(\Delta x\sum_{l=0}^{N-1}|u_l^n|^2\right)^{\frac{1}{2}}.$$

In addition, we define

$$D_tu_l^n=\frac{u_l^{n+1}-u_l^n}{\tau},\quad A_tu_l^n=\frac{u_l^{n+1}+u_l^n}{2},$$

as difference and average operators, respectively.

## 3 Energy-preserving wavelet method for the NLD equation

As we mentioned in Section 1, several numerical algorithms have been constructed for solving the NLD equation, however, most of which do not preserve energy conservation

https://doi.org/10.4208/aamm.2016.m1463 Published online by Cambridge University Press

law exactly. This section will present an energy-preserving algorithm and its corresponding conservative properties.

Applying the wavelet collocation method on space direction and midpoint rule on time direction in system (1.2), we obtain a scheme

$$\begin{cases} D_t\Psi_1^n + A_tB_1\Psi_2^n + \mathrm{i}mA_t\Psi_1^n + 2\mathrm{i}\lambda A_t(|\Psi_2^n|^2 - |\Psi_1^n|^2)\cdot A_t\Psi_1^n = 0, \\ D_t\Psi_2^n + A_tB_1\Psi_1^n - \mathrm{i}mA_t\Psi_2^n + 2\mathrm{i}\lambda A_t(|\Psi_1^n|^2 - |\Psi_2^n|^2)\cdot A_t\Psi_2^n = 0, \end{cases} \tag{3.1}$$

where

$$\Psi_1^n = (\psi_{1_0}^n, \psi_{1_1}^n, \cdots, \psi_{1_{N-1}}^n)^{\mathrm{T}}, \qquad \Psi_2^n = (\psi_{2_0}^n, \psi_{2_1}^n, \cdots, \psi_{2_{N-1}}^n)^{\mathrm{T}},$$
$$|\Psi_1^n|^2 = (|\psi_{1_0}^n|^2, |\psi_{1_1}^n|^2, \cdots, |\psi_{1_{N-1}}^n|^2)^{\mathrm{T}}, \qquad \Psi_1^n\cdot\Psi_2^n = (\psi_{1_0}^n\psi_{2_0}^n, \psi_{1_1}^n\psi_{2_1}^n, \cdots, \psi_{1_{N-1}}^n\psi_{2_{N-1}}^n)^{\mathrm{T}},$$

and so on.

**Theorem 3.1.** Under the periodic boundary conditions, the scheme (3.1) preserves the charge

$$\begin{aligned} \mathcal{Q}^{n+1} &= \|\Psi_1^{n+1}\|^2 + \|\Psi_2^{n+1}\|^2 = \Delta x \sum_{l=0}^{N-1} (|\psi_{1_l}^{n+1}|^2 + |\psi_{2_l}^{n+1}|^2) \\ &= \mathcal{Q}^n = \cdots = \mathcal{Q}^0. \end{aligned} \tag{3.2}$$

*Proof.* Making inner product of the first line of scheme (3.1) with $\Psi_1^{n+1} + \Psi_1^n$ follows

$$\begin{aligned} &\langle D_t\Psi_1^n, \Psi_1^{n+1} + \Psi_1^n\rangle + \langle A_tB_1\Psi_2^n, \Psi_1^{n+1} + \Psi_1^n\rangle + \mathrm{i}m\langle A_t\Psi_1^n, \Psi_1^{n+1} + \Psi_1^n\rangle \\ &\quad + 2\mathrm{i}\lambda\langle A_t(|\Psi_2^n|^2 - |\Psi_1^n|^2)\cdot A_t\Psi_1^n, \Psi_1^{n+1} + \Psi_1^n\rangle = 0. \end{aligned} \tag{3.3}$$

The first term is equivalent to

$$\frac{1}{\tau}\langle \Psi_1^{n+1} - \Psi_1^n, \Psi_1^{n+1} + \Psi_1^n\rangle = \frac{1}{\tau}(\|\Psi_1^{n+1}\|^2 - \|\Psi_1^n\|^2 + 2\mathrm{i}\Im\langle \Psi_1^{n+1}, \Psi_1^n\rangle). \tag{3.4}$$

The second term can be written as

$$\langle A_tB_1\Psi_2^n, \Psi_1^{n+1} + \Psi_1^n\rangle = 2\langle B_1A_t\Psi_2^n, A_t\Psi_1^n\rangle. \tag{3.5}$$

The third term

$$\mathrm{i}m\langle A_t\Psi_1^n, \Psi_1^{n+1} + \Psi_1^n\rangle = \frac{\mathrm{i}m}{2}\|\Psi_1^{n+1} + \Psi_1^n\|^2 \tag{3.6}$$

is purely imaginary. The last term

$$\begin{aligned} &2\mathrm{i}\lambda\langle A_t(|\Psi_2^n|^2 - |\Psi_1^n|^2)\cdot A_t\Psi_1^n, \Psi_1^{n+1} + \Psi_1^n\rangle \\ =&4\mathrm{i}\lambda\Delta x \sum_{l=0}^{N-1} A_t(|\psi_{2_l}^n|^2 - |\psi_{1_l}^n|^2)(A_t\psi_{1_l}^n)(A_t\overline{\psi_{1_l}^n}) \\ =&4\mathrm{i}\lambda\Delta x \sum_{l=0}^{N-1} A_t(|\psi_{2_l}^n|^2 - |\psi_{1_l}^n|^2)|A_t\psi_{1_l}^n|^2 \end{aligned} \tag{3.7}$$

https://doi.org/10.4208/aamm.2016.m1463 Published online by Cambridge University Press

is also purely imaginary. Then, we take the real part of Eq. (3.3) and obtain

$$\frac{1}{\tau}(\|\Psi_1^{n+1}\|^2-\|\Psi_1^n\|^2)+2\Re\langle B_1A_t\Psi_2^n,A_t\Psi_1^n\rangle=0, \tag{3.8}$$

where $\Re$ stands for the real part. Similarly, making inner product of the second line of scheme (3.1) with $\Psi_2^{n+1}+\Psi_2^n$ and taking the real part imply

$$\frac{1}{\tau}(\|\Psi_2^{n+1}\|^2-\|\Psi_2^n\|^2)+2\Re\langle B_1A_t\Psi_1^n,A_t\Psi_2^n\rangle=0. \tag{3.9}$$

We notice that $B_1$ is a real skew-symmetric matrix, hence

$$\begin{aligned}&\langle B_1A_t\Psi_2^n,A_t\Psi_1^n\rangle+\langle B_1A_t\Psi_1^n,A_t\Psi_2^n\rangle\\ =&\langle B_1A_t\Psi_2^n,A_t\Psi_1^n\rangle-\langle A_t\Psi_1^n,B_1A_t\Psi_2^n\rangle\\ =&2\mathrm{i}\Im\langle B_1A_t\Psi_2^n,A_t\Psi_1^n\rangle\end{aligned} \tag{3.10}$$

is purely imaginary. Combining Eqs. (3.8), (3.9) and (3.10) indicates

$$\|\Psi_1^{n+1}\|^2+\|\Psi_2^{n+1}\|^2=\|\Psi_1^n\|^2+\|\Psi_2^n\|^2. \tag{3.11}$$

Thus, we complete the proof. □

**Theorem 3.2.** Under the periodic boundary conditions, the scheme (3.1) satisfies the discrete energy conservation law

$$\begin{aligned}&\frac{\lambda}{2}\Delta x\sum_{l=0}^{N-1}(|\psi_1^{n+1}|^2-|\psi_2^{n+1}|^2)^2-\frac{m}{2}(\|\Psi_1^{n+1}\|^2-\|\Psi_2^{n+1}\|^2)\\ &\quad-\frac{\Delta x}{2}\sum_{l=0}^{N-1}\Big[q_{1_l}^{n+1}(B_1\mathbf{q}_4^{n+1})_l-q_{2_l}^{n+1}(B_1\mathbf{q}_3^{n+1})_l+q_{3_l}^{n+1}(B_1\mathbf{q}_2^{n+1})_l-q_{4_l}^{n+1}(B_1\mathbf{q}_1^{n+1})_l\Big]\\ =&\frac{\lambda}{2}\Delta x\sum_{l=0}^{N-1}(|\psi_1^n|^2-|\psi_2^n|^2)^2-\frac{m}{2}(\|\Psi_1^n\|^2-\|\Psi_2^n\|^2)\\ &\quad-\frac{\Delta x}{2}\sum_{l=0}^{N-1}\Big[q_{1_l}^n(B_1\mathbf{q}_4^n)_l-q_{2_l}^n(B_1\mathbf{q}_3^n)_l+q_{3_l}^n(B_1\mathbf{q}_2^n)_l-q_{4_l}^n(B_1\mathbf{q}_1^n)_l\Big].\end{aligned} \tag{3.12}$$

In other words

$$\mathcal{E}^{n+1}=\mathcal{E}^n=\cdots=\mathcal{E}^0. \tag{3.13}$$

*Proof.* Taking inner product of the first line of scheme (3.1) with $\Psi_1^{n+1}-\Psi_1^n$ follows

$$\begin{aligned}&\langle D_t\Psi_1^n,\Psi_1^{n+1}-\Psi_1^n\rangle+\langle A_tB_1\Psi_2^n,\Psi_1^{n+1}-\Psi_1^n\rangle+\mathrm{i}m\langle A_t\Psi_1^n,\Psi_1^{n+1}-\Psi_1^n\rangle\\ &\quad+2\mathrm{i}\lambda\langle A_t(|\Psi_2^n|^2-|\Psi_1^n|^2)\cdot A_t\Psi_1^n,\Psi_1^{n+1}-\Psi_1^n\rangle=0.\end{aligned} \tag{3.14}$$

https://doi.org/10.4208/aamm.2016.m1463 Published online by Cambridge University Press

The first term

$$\frac{1}{\tau}\langle\Psi_1^{n+1}-\Psi_1^n,\Psi_1^{n+1}-\Psi_1^n\rangle=\frac{1}{\tau}(\|\Psi_1^{n+1}-\Psi_1^n\|^2) \tag{3.15}$$

is a real function. The second term can be written as

$$\begin{aligned}
&\langle A_t B_1\Psi_2^n,\Psi_1^{n+1}-\Psi_1^n\rangle=\frac{1}{2}\langle B_1(\Psi_2^{n+1}+\Psi_2^n),\Psi_1^{n+1}-\Psi_1^n\rangle\\
=&\frac{\Delta x}{2}\sum_{l=0}^{N-1}\left[(B_1\Psi_2^{n+1})_l\overline{\psi_{1_l}^{n+1}}-(B_1\Psi_2^n)_l\overline{\psi_{1_l}^n}\right]+\frac{1}{2}(\langle B_1\Psi_2^n,\Psi_1^{n+1}\rangle-\langle B_1\Psi_2^{n+1},\Psi_1^n\rangle)\\
=&\frac{\Delta x}{2}\sum_{l=0}^{N-1}\Big[q_{1_l}^{n+1}(B_1\mathbf{q}_3^{n+1})_l+q_{2_l}^{n+1}(B_1\mathbf{q}_4^{n+1})_l-q_{1_l}^n(B_1\mathbf{q}_3^n)_l-q_{2_l}^n(B_1\mathbf{q}_4^n)_l\\
&+\mathrm{i}\Big(q_{1_l}^{n+1}(B_1\mathbf{q}_4^{n+1})_l-q_{2_l}^{n+1}(B_1\mathbf{q}_3^{n+1})_l-q_{1_l}^n(B_1\mathbf{q}_4^n)_l+q_{2_l}^n(B_1\mathbf{q}_3^n)_l\Big)\Big]\\
&+\frac{1}{2}(\langle B_1\Psi_2^n,\Psi_1^{n+1}\rangle-\langle B_1\Psi_2^{n+1},\Psi_1^n\rangle).
\end{aligned} \tag{3.16}$$

The third term is equivalent to

$$\begin{aligned}
&\frac{\mathrm{i}m}{2}\langle\Psi_1^{n+1}+\Psi_1^n,\Psi_1^{n+1}-\Psi_1^n\rangle\\
=&\frac{\mathrm{i}m}{2}(\|\Psi_1^{n+1}\|^2-\|\Psi_1^n\|^2+2\mathrm{i}\Im\langle\Psi_1^n,\Psi_1^{n+1}\rangle).
\end{aligned} \tag{3.17}$$

The last term is

$$\begin{aligned}
&2\mathrm{i}\lambda\langle A_t(|\Psi_2^n|^2-|\Psi_1^n|^2)\cdot A_t\Psi_1^n,\Psi_1^{n+1}-\Psi_1^n\rangle\\
=&\mathrm{i}\lambda\Delta x\sum_{l=0}^{N-1}A_t(|\psi_{2_l}^n|^2-|\psi_{1_l}^n|^2)\cdot(|\psi_{1_l}^{n+1}|^2-|\psi_{1_l}^n|^2+2\mathrm{i}\Im(\psi_{1_l}^n\overline{\psi_{1_l}^{n+1}}))\\
=&\frac{\mathrm{i}\lambda}{2}\Delta x\sum_{l=0}^{N-1}\big[(|\psi_{2_l}^{n+1}|^2-|\psi_{1_l}^{n+1}|^2)|\psi_{1_l}^{n+1}|^2-(|\psi_{2_l}^n|^2-|\psi_{1_l}^n|^2)|\psi_{1_l}^n|^2\\
&+(|\psi_{2_l}^n|^2-|\psi_{1_l}^n|^2)|\psi_{1_l}^{n+1}|^2-(|\psi_{2_l}^{n+1}|^2-|\psi_{1_l}^{n+1}|^2)|\psi_{1_l}^n|^2\\
&+4\mathrm{i}A_t(|\psi_{2_l}^n|^2-|\psi_{1_l}^n|^2)\cdot\Im(\psi_{1_l}^n\overline{\psi_{1_l}^{n+1}})\big].
\end{aligned} \tag{3.18}$$

Then, we take the imaginary part of Eq. (3.14) and obtain

$$\begin{aligned}
&\frac{\lambda}{2}\Delta x\sum_{l=0}^{N-1}\big[(|\psi_{2_l}^{n+1}|^2-|\psi_{1_l}^{n+1}|^2)|\psi_{1_l}^{n+1}|^2-(|\psi_{2_l}^n|^2-|\psi_{1_l}^n|^2)|\psi_{1_l}^n|^2\\
&+(|\psi_{2_l}^n|^2-|\psi_{1_l}^n|^2)|\psi_{1_l}^{n+1}|^2-(|\psi_{2_l}^{n+1}|^2-|\psi_{1_l}^{n+1}|^2)|\psi_{1_l}^n|^2\big]\\
&+\frac{m}{2}(\|\Psi_1^{n+1}\|^2-\|\Psi_1^n\|^2)+\frac{1}{2}\Im(\langle B_1\Psi_2^n,\Psi_1^{n+1}\rangle-\langle B_1\Psi_2^{n+1},\Psi_1^n\rangle)\\
&+\frac{\Delta x}{2}\sum_{l=0}^{N-1}\Big[q_{1_l}^{n+1}(B_1\mathbf{q}_4^{n+1})_l-q_{2_l}^{n+1}(B_1\mathbf{q}_3^{n+1})_l-q_{1_l}^n(B_1\mathbf{q}_4^n)_l+q_{2_l}^n(B_1\mathbf{q}_3^n)_l\Big]=0.
\end{aligned} \tag{3.19}$$

https://doi.org/10.4208/aamm.2016.m1463 Published online by Cambridge University Press

Similarly, making inner product of the second line of scheme (3.1) with $\Psi_2^{n+1}-\Psi_2^n$ and taking the imaginary part imply

$$\begin{aligned}
&\frac{\lambda}{2}\Delta x\sum_{l=0}^{N-1}\big[(|\psi_{1_l}^{n+1}|^2-|\psi_{2_l}^{n+1}|^2)|\psi_{2_l}^{n+1}|^2-(|\psi_{1_l}^{n}|^2-|\psi_{2_l}^{n}|^2)|\psi_{2_l}^{n}|^2\\
&\quad+(|\psi_{1_l}^{n}|^2-|\psi_{2_l}^{n}|^2)|\psi_{2_l}^{n+1}|^2-(|\psi_{1_l}^{n+1}|^2-|\psi_{2_l}^{n+1}|^2)|\psi_{2_l}^{n}|^2\big]\\
&\quad-\frac{m}{2}(\|\Psi_2^{n+1}\|^2-\|\Psi_2^n\|^2)+\frac{1}{2}\Im(\langle B_1\Psi_1^n,\Psi_2^{n+1}\rangle-\langle B_1\Psi_1^{n+1},\Psi_2^n\rangle)\\
&\quad+\frac{\Delta x}{2}\sum_{l=0}^{N-1}\Big[q_{3_l}^{n+1}(B_1\mathbf{q}_2^{n+1})_l-q_{4_l}^{n+1}(B_1\mathbf{q}_1^{n+1})_l-q_{3_l}^{n}(B_1\mathbf{q}_2^{n})_l+q_{4_l}^{n}(B_1\mathbf{q}_1^{n})_l\Big]=0.
\end{aligned}\tag{3.20}$$

We notice that

$$\begin{aligned}
&\langle B_1\Psi_2^n,\Psi_1^{n+1}\rangle-\langle B_1\Psi_2^{n+1},\Psi_1^n\rangle+\langle B_1\Psi_1^n,\Psi_2^{n+1}\rangle-\langle B_1\Psi_1^{n+1},\Psi_2^n\rangle\\
=&\langle B_1\Psi_2^n,\Psi_1^{n+1}\rangle+\langle\Psi_1^{n+1},B_1\Psi_2^n\rangle+\langle\Psi_2^{n+1},B_1\Psi_1^n\rangle+\langle B_1\Psi_1^n,\Psi_2^{n+1}\rangle\\
=&2\Re\langle B_1\Psi_2^n,\Psi_1^{n+1}\rangle+2\Re\langle\Psi_2^{n+1},B_1\Psi_1^n\rangle
\end{aligned}\tag{3.21}$$

is a real function. Combining Eqs. (3.19), (3.20) and (3.21) yields the discrete global energy conservation law (3.12). □

Both of the two properties reveal the stability of the EPW method applied to the NLD equation in the sense of the charge and energy conservation laws, and guarantee the effectiveness of the EPW method during long-time numerical computations.

## 4 Multi-symplectic wavelet integrators for the NLD equation

Compared with symplectic integrators for the Hamiltonian ordinary differential equations, the structure-preserving algorithms for Hamiltonian PDEs are comparatively less. By introducing the concept of multi-symplectic, this issue could be solved appropriately. Up to now, various typical multi-symplectic integrators [9, 21–26, 28–35] have been proposed for multi-symplectic Hamiltonian systems, which can preserve the discrete multi-symplectic conservation laws characterizing the spatial changes of the discrete symplectic structure. In this section, we first construct the multi-symplectic wavelet method and investigate its conservative properties. By taking the splitting technique and symplectic Euler method into the multi-symplectic integrator, we propose two efficient multi-symplectic algorithms, which would greatly reduce the computational cost.

Actually, the system (1.3) can be written as the Hamiltonian PDEs

$$Mz_t+Kz_x=\nabla_z S(z),\tag{4.1}$$

https://doi.org/10.4208/aamm.2016.m1463 Published online by Cambridge University Press

where

$$M=\begin{pmatrix} 0 & 1 & 0 & 0 \\ -1 & 0 & 0 & 0 \\ 0 & 0 & 0 & 1 \\ 0 & 0 & -1 & 0 \end{pmatrix}, \quad K=\begin{pmatrix} 0 & 0 & 0 & 1 \\ 0 & 0 & -1 & 0 \\ 0 & 1 & 0 & 0 \\ -1 & 0 & 0 & 0 \end{pmatrix},$$

$z=(q_1,q_2,q_3,q_4)^{\mathrm{T}}$ and the Hamiltonian function is

$$S(z)=\frac{1}{2}[\lambda(q_1^2+q_2^2-q_3^2-q_4^2)-m](q_1^2+q_2^2-q_3^2-q_4^2).$$

We can prove (4.1) has multi-symplectic conservation law [9]

$$\omega_t+\kappa_x=0 \tag{4.2}$$

with

$$\omega=\frac{1}{2}dz\wedge Mdz, \quad \kappa=\frac{1}{2}dz\wedge Kdz.$$

In addition, when $S(z)$ is independent of $x$ and $t$, the system (4.1) has local energy conservation law

$$E_t+F_x=0 \tag{4.3}$$

with

$$E(z)=S(z)-\frac{1}{2}z^{\mathrm{T}}Kz_x, \quad F(z)=\frac{1}{2}z^{\mathrm{T}}Kz_t,$$

and local momentum conservation law

$$I_t+G_x=0 \tag{4.4}$$

with

$$I(z)=\frac{1}{2}z^{\mathrm{T}}Mz_x, \quad G(z)=S(z)-\frac{1}{2}z^{\mathrm{T}}Mz_t.$$

For the NLD equation (1.2), the above conservation laws are given by

$$E(z)=S(z)-\frac{1}{2}\left(q_1\frac{\partial}{\partial x}q_4-q_2\frac{\partial}{\partial x}q_3+q_3\frac{\partial}{\partial x}q_2-q_4\frac{\partial}{\partial x}q_1\right), \tag{4.5a}$$

$$F(z)=\frac{1}{2}\left(q_1\frac{\partial}{\partial t}q_4-q_2\frac{\partial}{\partial t}q_3+q_3\frac{\partial}{\partial t}q_2-q_4\frac{\partial}{\partial t}q_1\right), \tag{4.5b}$$

$$I(z)=\frac{1}{2}\left(q_1\frac{\partial}{\partial x}q_2-q_2\frac{\partial}{\partial x}q_1+q_3\frac{\partial}{\partial x}q_4-q_4\frac{\partial}{\partial x}q_3\right), \tag{4.5c}$$

$$G(z)=S(z)-\frac{1}{2}\left(q_1\frac{\partial}{\partial t}q_2-q_2\frac{\partial}{\partial t}q_1+q_3\frac{\partial}{\partial t}q_4-q_4\frac{\partial}{\partial t}q_3\right). \tag{4.5d}$$

https://doi.org/10.4208/aamm.2016.m1463 Published online by Cambridge University Press

### 4.1 Multi-symplectic wavelet method

We apply wavelet collocation method on space direction and symplectic midpoint rule on time direction for the multi-symplectic PDEs (4.1), and obtain the MSW scheme

$$MD_t z_l^n + K\sum_{m=l-(M-1)}^{l+(M-1)} (B_1)_{l,m}(A_t z_m^n) = \nabla_z S(A_t z_l^n). \tag{4.6}$$

For the NLD equation (1.3), the scheme (4.6) can be rewritten as

$$\begin{cases} D_t\mathbf{q}_1^n + A_tB_1\mathbf{q}_3^n - mA_t\mathbf{q}_2^n - 2\lambda(|A_t\mathbf{q}_3^n|^2+|A_t\mathbf{q}_4^n|^2-|A_t\mathbf{q}_1^n|^2-|A_t\mathbf{q}_2^n|^2)\cdot A_t\mathbf{q}_2^n = 0,\\ D_t\mathbf{q}_2^n + A_tB_1\mathbf{q}_4^n + mA_t\mathbf{q}_1^n + 2\lambda(|A_t\mathbf{q}_3^n|^2+|A_t\mathbf{q}_4^n|^2-|A_t\mathbf{q}_1^n|^2-|A_t\mathbf{q}_2^n|^2)\cdot A_t\mathbf{q}_1^n = 0,\\ D_t\mathbf{q}_3^n + A_tB_1\mathbf{q}_1^n + mA_t\mathbf{q}_4^n + 2\lambda(|A_t\mathbf{q}_3^n|^2+|A_t\mathbf{q}_4^n|^2-|A_t\mathbf{q}_1^n|^2-|A_t\mathbf{q}_2^n|^2)\cdot A_t\mathbf{q}_4^n = 0,\\ D_t\mathbf{q}_4^n + A_tB_1\mathbf{q}_2^n - mA_t\mathbf{q}_3^n - 2\lambda(|A_t\mathbf{q}_3^n|^2+|A_t\mathbf{q}_4^n|^2-|A_t\mathbf{q}_1^n|^2-|A_t\mathbf{q}_2^n|^2)\cdot A_t\mathbf{q}_3^n = 0, \end{cases} \tag{4.7}$$

or

$$\begin{cases} D_t\Psi_1^n + A_tB_1\Psi_2^n + \mathrm{i}mA_t\Psi_1^n + 2\mathrm{i}\lambda(|A_t\Psi_2^n|^2-|A_t\Psi_1^n|^2)\cdot A_t\Psi_1^n = 0,\\ D_t\Psi_2^n + A_tB_1\Psi_1^n - \mathrm{i}mA_t\Psi_2^n + 2\mathrm{i}\lambda(|A_t\Psi_1^n|^2-|A_t\Psi_2^n|^2)\cdot A_t\Psi_2^n = 0, \end{cases} \tag{4.8}$$

where

$$|A_t\Psi_1^n|^2 = |A_t\mathbf{q}_1^n|^2+|A_t\mathbf{q}_2^n|^2, \quad |A_t\Psi_2^n|^2 = |A_t\mathbf{q}_3^n|^2+|A_t\mathbf{q}_4^n|^2.$$

Making use of the variational equations of Eq. (4.6), we have the following theorem [12].

**Theorem 4.1.** The MSW scheme (4.6) satisfies $N$ full discrete multi-symplectic conservation laws

$$D_t\omega_l^n + \sum_{m=l-(M-1)}^{l+(M-1)} (B_1)_{l,m}(A_t\kappa_{l,m}^n) = 0, \tag{4.9}$$

where

$$\omega_l^n = \frac{1}{2}(dz_l^n \wedge Mdz_l^n), \quad A_t\kappa_{l,m}^n = dA_tz_l^n \wedge KdA_tz_m^n, \quad l = 0,1,\cdots,N-1.$$

The residual of the discrete local energy conservation law for the MSW method (4.7) or (4.8) is

$$RE^n = D_tE^n + B_1A_tF^n, \tag{4.10}$$

where

$$\begin{aligned} E^n &= \frac{\lambda}{2}(|\mathbf{q}_2^n|^2+|\mathbf{q}_1^n|^2-|\mathbf{q}_4^n|^2-|\mathbf{q}_3^n|^2)^2 - \frac{m}{2}(|\mathbf{q}_2^n|^2+|\mathbf{q}_1^n|^2-|\mathbf{q}_4^n|^2-|\mathbf{q}_3^n|^2)\\ &\quad -\frac{1}{2}\Big[\mathbf{q}_1^n\cdot(B_1\mathbf{q}_4^n) - \mathbf{q}_2^n\cdot(B_1\mathbf{q}_3^n) + \mathbf{q}_3^n\cdot(B_1\mathbf{q}_2^n) - \mathbf{q}_4^n\cdot(B_1\mathbf{q}_1^n)\Big],\\ A_tF^n &= \frac{1}{2}\Big[(A_t\mathbf{q}_1^n)\cdot(D_t\mathbf{q}_4^n) - (A_t\mathbf{q}_2^n)\cdot(D_t\mathbf{q}_3^n) + (A_t\mathbf{q}_3^n)\cdot(D_t\mathbf{q}_2^n) - (A_t\mathbf{q}_4^n)\cdot(D_t\mathbf{q}_1^n)\Big], \end{aligned}$$

https://doi.org/10.4208/aamm.2016.m1463 Published online by Cambridge University Press

and the residual of the discrete local momentum conservation law is

$$RM^n = D_t I^n + B_1 A_t G^n, \tag{4.11}$$

where

$$\begin{aligned}
I^n =& \frac{1}{2}\Big[\mathbf{q}_1^n\cdot(B_1\mathbf{q}_2^n)-\mathbf{q}_2^n\cdot(B_1\mathbf{q}_1^n)+\mathbf{q}_3^n\cdot(B_1\mathbf{q}_4^n)-\mathbf{q}_4^n\cdot(B_1\mathbf{q}_3^n)\Big],\\
A_tG^n =& \frac{\lambda}{2}(|A_t\mathbf{q}_2^n|^2+|A_t\mathbf{q}_1^n|^2-|A_t\mathbf{q}_4^n|^2-|A_t\mathbf{q}_3^n|^2)^2-\frac{m}{2}(|A_t\mathbf{q}_2^n|^2+|A_t\mathbf{q}_1^n|^2\\
&-|A_t\mathbf{q}_4^n|^2-|A_t\mathbf{q}_3^n|^2)-\frac{1}{2}\Big[(A_t\mathbf{q}_1^n)\cdot(D_t\mathbf{q}_2^n)-(A_t\mathbf{q}_2^n)\cdot(D_t\mathbf{q}_1^n)\\
&+(A_t\mathbf{q}_3^n)\cdot(D_t\mathbf{q}_4^n)-(A_t\mathbf{q}_4^n)\cdot(D_t\mathbf{q}_3^n)\Big].
\end{aligned}$$

Since the Hamiltonian function $S(z)$ is biquadratic in $z$, the MSW scheme (4.7) or (4.8) does not conserve the discrete local conservation laws exactly [9].

Comparing with the energy conservation law, we obtain the following error estimation

**Theorem 4.2.** The MSW scheme (4.7) or (4.8) satisfies the following error estimation

$$\begin{aligned}
&A_t\mathcal{E}^{n+1}-A_t\mathcal{E}^n\\
=&\frac{\lambda}{2}\Delta x\sum_{l=0}^{N-1}(|A_t\psi_{1_l}^{n+1}|^2-|A_t\psi_{2_l}^{n+1}|^2+|A_t\psi_{1_l}^{n}|^2-|A_t\psi_{2_l}^{n}|^2)\cdot\Im(A_t\psi_{1_l}^{n+1}\overline{A_t\psi_{1_l}^{n}}-A_t\psi_{2_l}^{n+1}\overline{A_t\psi_{2_l}^{n}})\\
=&\mathcal{O}(\tau^4),
\end{aligned}\tag{4.12}$$

where

$$\begin{aligned}
A_t\mathcal{E}^n =& \frac{\lambda}{2}\Delta x\sum_{l=0}^{N-1}(|A_t\psi_{1_l}^{n}|^2-|A_t\psi_{2_l}^{n}|^2)^2-\frac{m}{2}(\|A_t\Psi_1^n\|^2-\|A_t\Psi_2^n\|^2)\\
&-\frac{1}{2}\Im(\langle B_1A_t\Psi_2^n,A_t\Psi_1^n\rangle+\langle B_1A_t\Psi_1^n,A_t\Psi_2^n\rangle).
\end{aligned}$$

*Proof.* The first line of scheme (4.8) is equivalent to

$$D_tA_t\Psi_1^n+A_t^2B_1\Psi_2^n+\mathrm{i}mA_t^2\Psi_1^n+2\mathrm{i}\lambda A_t[(|A_t\Psi_2^n|^2-|A_t\Psi_1^n|^2)\cdot A_t\Psi_1^n]=0. \tag{4.13}$$

Making inner product with the vector $A_tD_t\Psi_1^n$ for (4.13) and taking the imaginary part, we obtain

$$\begin{aligned}
&\frac{\lambda}{2}\Delta x\sum_{l=0}^{N-1}\big[(|A_t\psi_{2_l}^{n+1}|^2-|A_t\psi_{1_l}^{n+1}|^2)|A_t\psi_{1_l}^{n+1}|^2-(|A_t\psi_{2_l}^{n}|^2-|A_t\psi_{1_l}^{n}|^2)|A_t\psi_{1_l}^{n}|^2\\
&+(|A_t\psi_{2_l}^{n}|^2-|A_t\psi_{1_l}^{n}|^2+|A_t\psi_{2_l}^{n+1}|^2-|A_t\psi_{1_l}^{n+1}|^2)\cdot\Im(A_t\psi_{1_l}^{n}\overline{A_t\psi_{1_l}^{n+1}})\big]\\
&+\frac{m}{2}(\|A_t\Psi_1^{n+1}\|^2-\|A_t\Psi_1^{n}\|^2)+\frac{1}{2}\Im(\langle B_1A_t\Psi_2^n,A_t\Psi_1^{n+1}\rangle-\langle B_1A_t\Psi_2^{n+1},A_t\Psi_1^{n}\rangle)\\
&+\frac{1}{2}\Im(\langle B_1A_t\Psi_2^{n+1},A_t\Psi_1^{n+1}\rangle-\langle B_1A_t\Psi_2^{n},A_t\Psi_1^{n}\rangle)=0.
\end{aligned}\tag{4.14}$$

https://doi.org/10.4208/aamm.2016.m1463 Published online by Cambridge University Press

Similarly, implementing the analogical process on the second line scheme (4.8) yields

$$\begin{aligned}
&\frac{\lambda}{2}\Delta x\sum_{l=0}^{N-1}\big[(|A_t\psi_{1_l}^{n+1}|^2-|A_t\psi_{2_l}^{n+1}|^2)|A_t\psi_{2_l}^{n+1}|^2-(|A_t\psi_{1_l}^{n}|^2-|A_t\psi_{2_l}^{n}|^2)|A_t\psi_{2_l}^{n}|^2\\
&\quad+(|A_t\psi_{1_l}^{n}|^2-|A_t\psi_{2_l}^{n}|^2+|A_t\psi_{1_l}^{n+1}|^2-|A_t\psi_{2_l}^{n+1}|^2)\cdot\Im(A_t\psi_{2_l}^{n}\overline{A_t\psi_{2_l}^{n+1}})\big]\\
&\quad-\frac{m}{2}(\|A_t\Psi_2^{n+1}\|^2-\|A_t\Psi_2^{n}\|^2)+\frac{1}{2}\Im(\langle B_1A_t\Psi_1^{n},A_t\Psi_2^{n+1}\rangle-\langle B_1A_t\Psi_1^{n+1},A_t\Psi_2^{n}\rangle)\\
&\quad+\frac{1}{2}\Im(\langle B_1A_t\Psi_1^{n+1},A_t\Psi_2^{n+1}\rangle-\langle B_1A_t\Psi_1^{n},A_t\Psi_2^{n}\rangle)=0.
\end{aligned}\tag{4.15}$$

Summing Eqs. (4.14) and (4.15) implies (4.12). □

Making inner product of the first line of scheme (4.8) with $\Psi_1^{n+1}+\Psi_1^n$, and the second one with $\Psi_2^{n+1}+\Psi_2^n$, then taking the real part like Theorem 3.1, we can easily obtain

**Theorem 4.3.** Under the periodic boundary conditions, the scheme (4.7) or (4.8) preserves the charge

$$\begin{aligned}
\mathcal{Q}^{n+1}&=\|\Psi_1^{n+1}\|^2+\|\Psi_2^{n+1}\|^2\\
&=\Delta x\sum_{l=0}^{N-1}(|\psi_{1_l}^{n+1}|^2+|\psi_{2_l}^{n+1}|^2)\\
&=\mathcal{Q}^n=\cdots=\mathcal{Q}^0.
\end{aligned}\tag{4.16}$$

## 4.2 Accelerated strategies for the multi-symplectic integrator

The multi-symplectic system (4.1) can be split into sub-multi-symplectic systems

$$Mz_t+K_iz_x=\nabla_zS^i(z),\quad i=1,2,\cdots,N,\tag{4.17}$$

where

$$K=\sum_{i=1}^{N}K_i,\quad S(z)=\sum_{i=1}^{N}S^i(z),$$

which have the multi-symplectic conservation laws

$$\omega_t+\kappa_{ix}=0,\tag{4.18}$$

with

$$\omega=\frac{1}{2}dz\wedge Mdz,\quad \kappa_i=\frac{1}{2}dz\wedge K_idz,\quad i=1,2,\cdots,N.$$

https://doi.org/10.4208/aamm.2016.m1463 Published online by Cambridge University Press

For the NLD equation (1.2), it can be split into a linear subproblem

$$\mathcal{L}:\begin{cases}\dfrac{\partial}{\partial t}q_1+\dfrac{\partial}{\partial x}q_3-mq_2=0,\\ \dfrac{\partial}{\partial t}q_2+\dfrac{\partial}{\partial x}q_4+mq_1=0,\\ \dfrac{\partial}{\partial t}q_3+\dfrac{\partial}{\partial x}q_1+mq_4=0,\\ \dfrac{\partial}{\partial t}q_4+\dfrac{\partial}{\partial x}q_2-mq_3=0,\end{cases}\tag{4.19}$$

and a nonlinear subproblem

$$\mathcal{N}:\begin{cases}\dfrac{\partial}{\partial t}q_1-2\lambda(q_3^2+q_4^2-q_1^2-q_2^2)q_2=0,\\ \dfrac{\partial}{\partial t}q_2+2\lambda(q_3^2+q_4^2-q_1^2-q_2^2)q_1=0,\\ \dfrac{\partial}{\partial t}q_3+2\lambda(q_3^2+q_4^2-q_1^2-q_2^2)q_4=0,\\ \dfrac{\partial}{\partial t}q_4-2\lambda(q_3^2+q_4^2-q_1^2-q_2^2)q_3=0.\end{cases}\tag{4.20}$$

Both of the linear subproblem (4.19) and the nonlinear subproblem (4.20) can be written into multi-symplectic systems (4.17) with

$$\mathcal{L}:K_1=K,\qquad S^1(z)=-\frac{1}{2}m(q_1^2+q_2^2-q_3^2-q_4^2),$$
$$\mathcal{N}:K_2=\mathbf{0},\qquad S^2(z)=\frac{1}{2}\lambda(q_1^2+q_2^2-q_3^2-q_4^2)^2.$$

Furthermore, the nonlinear subproblem (4.20) can also be written as an infinite Hamiltonian system

$$z_t=J^{-1}\frac{\delta}{\delta z}H(z),\quad z=(q_1,q_2,q_3,q_4)^{\mathrm{T}},\tag{4.21}$$

with a symplectic conservation law

$$\frac{d}{dt}\omega=0,\tag{4.22}$$

where $J=M$, $\omega=\frac{1}{2}dz\wedge Mdz$ and the Hamiltonian function is

$$H(z)=\int\frac{1}{2}\lambda(q_1^2+q_2^2-q_3^2-q_4^2)^2dx.\tag{4.23}$$

Discreting the linear subsystem (4.19) by wavelet collocation method in space and mid-point scheme in time direction, we obtain the implicit scheme

$$\begin{cases}D_t\mathbf{q}_1^n+A_tB_1\mathbf{q}_3^n-mA_t\mathbf{q}_2^n=0,\\ D_t\mathbf{q}_2^n+A_tB_1\mathbf{q}_4^n+mA_t\mathbf{q}_1^n=0,\\ D_t\mathbf{q}_3^n+A_tB_1\mathbf{q}_1^n+mA_t\mathbf{q}_4^n=0,\\ D_t\mathbf{q}_4^n+A_tB_1\mathbf{q}_2^n-mA_t\mathbf{q}_3^n=0.\end{cases}\tag{4.24}$$

https://doi.org/10.4208/aamm.2016.m1463 Published online by Cambridge University Press

Furthermore, discreting Eq. (4.19) by symplectic Euler scheme [20] instead of mid-point scheme in time direction, we can obtain the semi-explicit scheme

$$\begin{cases} D_t\mathbf{q}_1^n+B_1\mathbf{q}_3^{n+1}-m\mathbf{q}_2^{n+1}=0, \\ D_t\mathbf{q}_2^n+B_1\mathbf{q}_4^n+m\mathbf{q}_1^n=0, \\ D_t\mathbf{q}_3^n+B_1\mathbf{q}_1^{n+1}+m\mathbf{q}_4^{n+1}=0, \\ D_t\mathbf{q}_4^n+B_1\mathbf{q}_2^n-m\mathbf{q}_3^n=0. \end{cases} \tag{4.25}$$

It is obvious that the scheme (4.25) for the linear subproblem (4.19) is semi-explicit, which means that we do not need to solve all of the nonlinear algebraic equations at every time step. Actually, the second and forth lines are entirely explicit, but the first and third lines need to solve nonlinear algebraic equation at every spatial grid.

For the nonlinear subproblem (4.20), we choose the mid-point implicit scheme in time direction. Then, we obtain a symplectic scheme for the nonlinear subproblem

$$\begin{cases} D_t\mathbf{q}_1^n-2\lambda(|A_t\mathbf{q}_3^n|^2+|A_t\mathbf{q}_4^n|^2-|A_t\mathbf{q}_1^n|^2-|A_t\mathbf{q}_2^n|^2)\cdot A_t\mathbf{q}_2^n=0, \\ D_t\mathbf{q}_2^n+2\lambda(|A_t\mathbf{q}_3^n|^2+|A_t\mathbf{q}_4^n|^2-|A_t\mathbf{q}_1^n|^2-|A_t\mathbf{q}_2^n|^2)\cdot A_t\mathbf{q}_1^n=0, \\ D_t\mathbf{q}_3^n+2\lambda(|A_t\mathbf{q}_3^n|^2+|A_t\mathbf{q}_4^n|^2-|A_t\mathbf{q}_1^n|^2-|A_t\mathbf{q}_2^n|^2)\cdot A_t\mathbf{q}_4^n=0, \\ D_t\mathbf{q}_4^n-2\lambda(|A_t\mathbf{q}_3^n|^2+|A_t\mathbf{q}_4^n|^2-|A_t\mathbf{q}_1^n|^2-|A_t\mathbf{q}_2^n|^2)\cdot A_t\mathbf{q}_3^n=0, \end{cases} \tag{4.26}$$

or

$$\begin{cases} D_t\Psi_1^n+2\mathrm{i}\lambda(|A_t\Psi_2^n|^2-|A_t\Psi_1^n|^2)\cdot A_t\Psi_1^n=0, \\ D_t\Psi_2^n+2\mathrm{i}\lambda(|A_t\Psi_1^n|^2-|A_t\Psi_2^n|^2)\cdot A_t\Psi_2^n=0. \end{cases} \tag{4.27}$$

In this paper, the solution may be advanced from one-time level to next by means of the following second-order formula [36]

$$u_i(x,t+\Delta t)=\exp\left(\frac{\Delta t}{2}\mathcal{N}\right)\exp(\Delta t\mathcal{L})\exp\left(\frac{\Delta t}{2}\mathcal{N}\right)u_i(x,t). \tag{4.28}$$

If the implicit scheme (4.24) is used for the linear subsystem, we refer to it as multi-symplectic wavelet splitting (MSWS1) method. Otherwise, we take it as semi-explicit multi-symplectic wavelet splitting (MSWS2) method, when semi-explicit scheme (4.25) is used. In fact, we can construct arbitrary order for the splitting technique. Many works [14–19] have verified that it would greatly decrease the cost in computations.

## 5 Numerical simulations

In the section, we conduct some typical numerical examples to show the effectiveness and high accuracy for proposed algorithms during long-time simulations. All of the solutions are computed with space-step $\Delta x=0.125$, time-step $\Delta t=0.01$ and periodic boundary conditions. The autocorrelation function AD30 [11] is used for wavelet collocation method

https://doi.org/10.4208/aamm.2016.m1463 Published online by Cambridge University Press

in following examples. In addition, we solve the implicit parts of the algorithms by using the fixed-point iteration method with tolerance $\varepsilon=10^{-30}$.

In addition, our proposed EPW and MSW methods are both mainly compared with "High-order Compact" finite difference method. We approximate the space derivative $\frac{d}{dx}\Phi$ by compact finite difference method, which yields

$$\alpha\Phi'_{j-1}+\Phi'_j+\alpha\Phi'_{j+1}=b_1\frac{\Phi_{j+2}-\Phi_{j-2}}{4h}+a_1\frac{\Phi_{j+1}-\Phi_{j-1}}{2h}, \tag{5.1}$$

where $\alpha$, $a_1$ and $b_1$ are constants that depend on the order condition constrains, $h$ is also the spatial step size. Especially in this section, we choose sixth-order accurate scheme [17], which yields

$$A\frac{d}{dx}\Phi=B\Phi,$$

where $A$ and $B$ are $N\times N$ circulant matrices with elements

$$A=Circ(3,1,0,\cdots,0,1),\quad B=Circ(0,28,1,0,\cdots,0,-1,-28).$$

In general, if the first row is $(c_1,c_2,\cdots,c_N)$, we denote the associated circulant matrix by $Circ(c_1,c_2,\cdots,c_N)$. Note that the $(m,n)$ entry of this matrix is $c_{n-m+1}$. Obviously, $A$ is symmetric and $B$ is skew-symmetric. Therefore, the first order differential operator $\partial_x$ yields a skew-symmetric differential matrix $D_1=A^{-1}B$. On the analogy of EPW and MSW methods, we use high-order compact finite difference method in spatial discretization and obtain the similar so called EPHC and MSHC methods likewise.

The errors in discrete charge, energy and momentum are defined by $\mathcal{Q}^n-\mathcal{Q}^0$, $-2\sum_{k=1}^N(E_k^n-E_k^0)\Delta x$, and $2\sum_{k=1}^N(I_k^n-I_k^0)\Delta x$, respectively, here, $E_k^n\approx E(z_k^n)$ and $I_k^n\approx I(z_k^n)$. We use $(B_1q_i^n)_k$ to approximate $\frac{\partial}{\partial x}q_{i_k}$ that appears in $E_k^n$ and $I_k^n$, respectively, $i=1,2,3,4$.

**Example 5.1.** We take the constants $m=1$ and $\lambda=\frac{1}{2}$ in (1.2), and the NLD equation has the following theoretical solitary wave solution [1]

$$\Psi^{sw}=(\Psi_1^{sw},\Psi_2^{sw})^{\mathrm{T}}=(M(x),iN(x))^{\mathrm{T}}e^{-\mathrm{i}\Lambda t}, \tag{5.2}$$

where

$$M(x)=(2(1-\Lambda^2))^{1/2}(1+\Lambda)^{1/2}\frac{\cosh((1-\Lambda^2)^{1/2}x)}{1+\Lambda\cosh(2(1-\Lambda^2)^{1/2}x)}, \tag{5.3a}$$

$$N(x)=(2(1-\Lambda^2))^{1/2}(1-\Lambda)^{1/2}\frac{\sinh((1-\Lambda^2)^{1/2}x)}{1+\Lambda\cosh(2(1-\Lambda^2)^{1/2}x)}, \tag{5.3b}$$

with the frequency $\Lambda=0.75$.

We solve the problem in spatial interval $[-24,24]$, which can make the lower parts of waves observable. In practice, the function $\Psi^{sw}$ is not mathematically periodic. Since the value is very close to zero near the boundary when the spatial interval is large enough, we

https://doi.org/10.4208/aamm.2016.m1463 Published online by Cambridge University Press

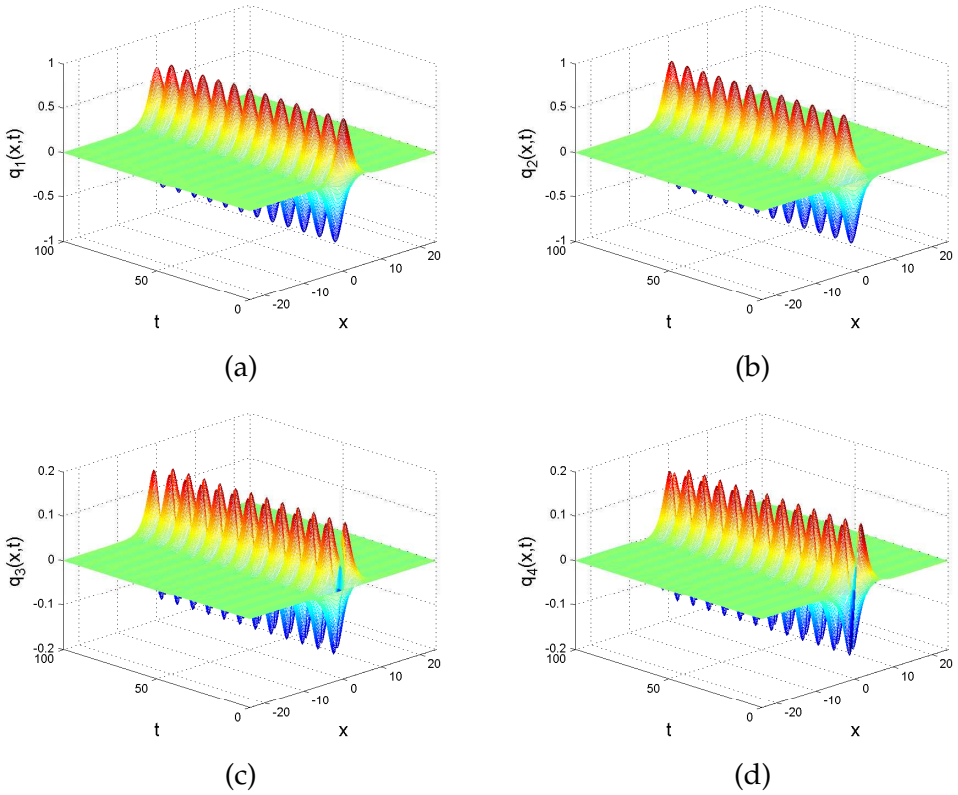



Figure 1: The four numerical solitary wave functions obtained by the MSW method: (a) $q_1(x,t)$; (b) $q_2(x,t)$; (c) $q_3(x,t)$; (d) $q_4(x,t)$.

can use the periodic boundary conditions for simplicity. The time interval $[0,100]$ contains almost 12 periods that match with the theoretical solution. The results of EPW, MSW, MSWS1 and MSWS2 are similar. Therefore, we only show the results of MSW in Fig. 1. Consequently, the plots in Fig. 1 show the periodic behavior almost perfectly. To measure the accuracy and efficiency of our methods, the $L^2$ and $L^\infty$ errors at different time, and the consumptions of CPU time as well, are displayed in Table 1. The results indicate that all of the four algorithms can simulate the solitary wave precisely. EPW and MSW have a little smaller errors than MSWS1 and MSWS2, and obviously EPW exhibits the best accuracies than the others. In detail, all the errors seem to show the feature of linear growth, which is typical for other conservative methods. In addition, it is observed that the splitting integrators are much more efficient than the former integrators. Furthermore, compared with implicit methods, the semi-explicit technique of the MSWS2 method takes much less CPU time. The discrete charge errors by proposed methods are shown in Fig. 2, which indicates that the four algorithms can preserve charge within roundoff errors of computer. Table 2 reveals that EPW, MSW, EPHC and MSHC have similar performances.

https://doi.org/10.4208/aamm.2016.m1463 Published online by Cambridge University Press

Table 1: Comparison of errors at different time and CPU time with the four algorithms.

| Time | $\Psi_1$ | | $\Psi_2$ | | CPU time (s) |
|---|---|---|---|---|---|
| | $L^2$ error | $L^\infty$ error | $L^2$error | $L^\infty$ error | |
| EPW method | | | | | |
| 20 | 2.204E-5 | 9.372E-6 | 4.922E-6 | 1.940E-6 | |
| 40 | 4.380E-5 | 2.343E-5 | 9.887E-6 | 4.747E-6 | |
| 60 | 6.530E-5 | 3.079E-5 | 1.485E-5 | 6.426E-6 | |
| 80 | 8.673E-5 | 4.505E-5 | 1.979E-5 | 9.169E-6 | |
| 100 | 1.086E-4 | 5.500E-5 | 2.470E-5 | 1.129E-5 | 4927 |
| MSW method | | | | | |
| 20 | 8.816E-5 | 3.748E-5 | 1.968E-5 | 7.761E-6 | |
| 40 | 1.753E-4 | 9.371E-5 | 3.951E-5 | 1.893E-5 | |
| 60 | 2.613E-4 | 1.231E-4 | 5.940E-5 | 2.565E-5 | |
| 80 | 3.470E-4 | 1.803E-4 | 7.916E-5 | 3.666E-5 | |
| 100 | 4.349E-4 | 2.200E-4 | 9.880E-5 | 4.517E-5 | 4858 |
| MSWS1 method | | | | | |
| 20 | 3.526E-4 | 1.499E-4 | 7.874E-5 | 3.104E-5 | |
| 40 | 7.014E-4 | 3.748E-4 | 1.580E-4 | 7.569E-5 | |
| 60 | 1.045E-3 | 4.924E-4 | 2.375E-4 | 1.025E-4 | |
| 80 | 1.388E-3 | 7.214E-4 | 3.166E-4 | 1.466E-4 | |
| 100 | 1.739E-3 | 8.800E-4 | 3.952E-4 | 1.806E-4 | 596 |
| MSWS2 method | | | | | |
| 20 | 3.526E-4 | 1.499E-4 | 7.874E-5 | 3.099E-5 | |
| 40 | 7.014E-4 | 3.748E-4 | 1.580E-4 | 7.562E-5 | |
| 60 | 1.045E-3 | 4.924E-4 | 2.375E-4 | 1.018E-4 | |
| 80 | 1.388E-3 | 7.214E-4 | 3.166E-4 | 1.465E-4 | |
| 100 | 1.739E-3 | 8.800E-4 | 3.952E-4 | 1.800E-4 | 73 |

Table 2: Comparison of errors at $T=100$.

| | Real part | | Imaginary part | |
|---|---|---|---|---|
| | $L^2$ error | $L^\infty$ error | $L^2$error | $L^\infty$ error |
| EPW method | 1.086E-4 | 5.500E-5 | 2.470E-5 | 1.129E-5 |
| EPHC method | 1.206E-4 | 6.810E-5 | 2.848E-5 | 1.366E-5 |
| MSW method | 4.349E-4 | 2.200E-4 | 9.880E-5 | 4.517E-5 |
| MSHC method | 4.437E-4 | 2.331E-4 | 1.011E-4 | 4.720E-5 |

Compared with the sixth-order compact finite difference methods, i.e., EPHC and MSHC, the errors, in some sense, of wavelet-based methods (EPW and MSW) seem a little less.

Fig. 3 and Fig. 4 show the corresponding errors in energy and momentum by EPW, MSW, EPHC and MSHC methods. We find that the discrete energy errors by EPW are preserved to an accuracy $10^{-12}$, and much better than those by the MSW method, which verify the theoretical analysis. The discrete momentum errors by EPW and MSW methods are both controlled in the scale of $10^{-16}$, that has been in the roundoff error of com-

https://doi.org/10.4208/aamm.2016.m1463 Published online by Cambridge University Press

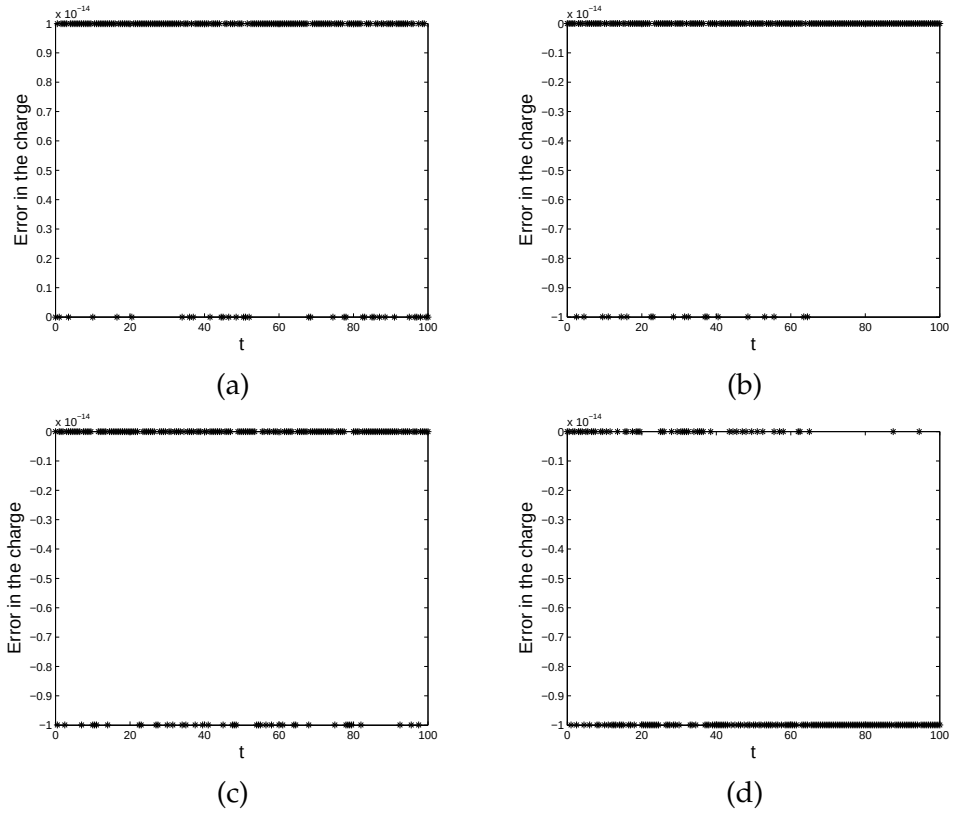



Figure 2: The errors in discrete charge: (a) EPW; (b) MSW; (c) MSWS1; (d) MSWS2.

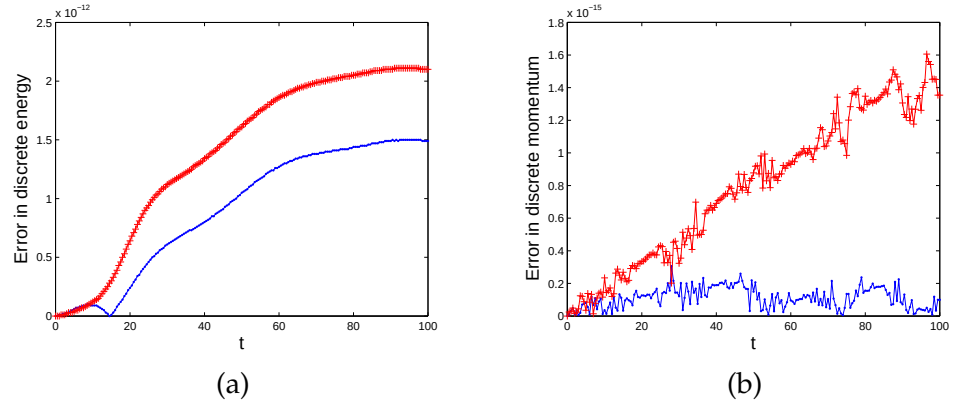
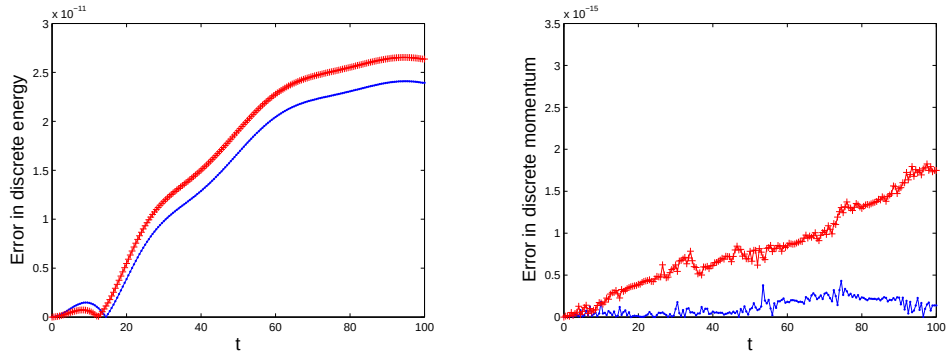



Figure 3: The errors in discrete energy and momentum. Blue · symbols: EPW; Red + symbols: EPHC.

puter. Meanwhile, Compared with EPHC and MSHC methods, the proposed EPW and MSW methods exhibit a little better. Moreover, the results by proposed methods, in some sense, are better than those obtained by the MSRK method in [1].

https://doi.org/10.4208/aamm.2016.m1463 Published online by Cambridge University Press




(a) (b)

Figure 4: The errors in discrete energy and momentum. Blue · symbols: MSW; Red + symbols: MSHC.

**Example 5.2.** The NLD equation (1.2) also has a single solitary wave solution [8] with a velocity $v$:

$$\Psi^{ss}=(\Psi_1^{ss}(x,t),\Psi_2^{ss}(x,t))^{\mathrm{T}}, \tag{5.4}$$

where

$$\Psi_1^{ss}(x,t)=\sqrt{\frac{\gamma+1}{2}}\Psi_1^{sw}(\tilde{x},\tilde{t})+\mathrm{sign}(v)\sqrt{\frac{\gamma-1}{2}}\Psi_2^{sw}(\tilde{x},\tilde{t}), \tag{5.5a}$$

$$\Psi_2^{ss}(x,t)=\sqrt{\frac{\gamma+1}{2}}\Psi_2^{sw}(\tilde{x},\tilde{t})+\mathrm{sign}(v)\sqrt{\frac{\gamma-1}{2}}\Psi_1^{sw}(\tilde{x},\tilde{t}). \tag{5.5b}$$

Here $\gamma=1/\sqrt{1-v^2}$, $\tilde{x}=\gamma(x-vt)$, $\tilde{t}=\gamma(t-vx)$, $\Psi_1^{sw}$ and $\Psi_2^{sw}$ are defined in (5.2) and $\mathrm{sign}(x)$ is the sign function. The function $\Psi^{ss}(x,t)$ represents a solitary wave traveling from left to right if $v>0$, or traveling from right to left if $v<0$, and a standing wave (5.2) if $v=0$. In addition, the charge density of the NLD equation (1.2) is defined by

$$\rho_Q(x,t)=|\Psi_1|^2+|\Psi_2|^2. \tag{5.6}$$

## Binary collisions

The collision of two solitons of the NLD model (1.2) is presented in Fig. 5 (obtained by the EPW method) with the initial data

$$\Psi(x,0)=\Psi_l^{ss}(x-x_l,0)+\Psi_r^{ss}(x-x_r,0). \tag{5.7}$$

It is seen that when $\Lambda=0.5$, the interaction of these solitons is elastic and two solitons keep their initial shapes and velocities after their collision. While $\Lambda=0.2$, the interaction is inelastic, oscillatory waves are generated after their collision. The discrete charge errors are shown in Fig. 6. From these graphs, one can see that the errors in charge are all within the roundoff error of machine, and do not exhibit any growth for the duration of the

https://doi.org/10.4208/aamm.2016.m1463 Published online by Cambridge University Press

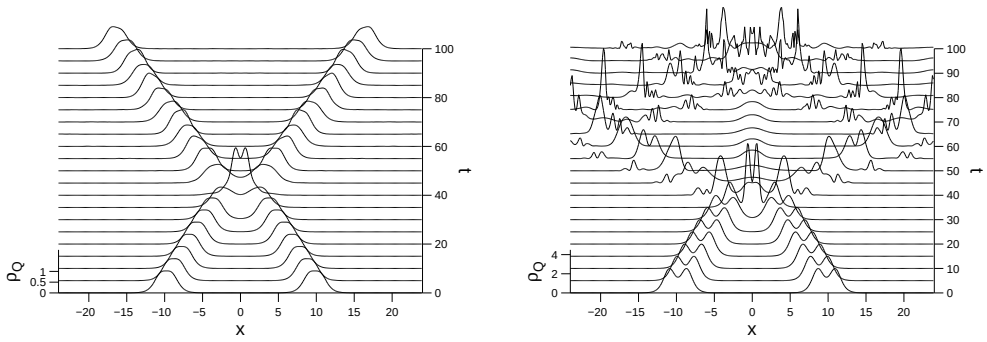



Figure 5: The collision of two solitons of the NLD model (1.2) by EPW with $v_l=-v_r=0.2$ and $x_r=-x_l=10$, $[x_L,x_R]=[-24,24]$. $\Lambda=0.5$ (a); $\Lambda=0.2$ (b).

simulation. The corresponding errors in energy and momentum are displayed in Fig. 7. It is clear that all the proposed structure-preserving methods conserve global energy and momentum exactly. In some sense, the energy-preserving ability of the EPW method is better than others. In addition, the CPU time by the MSWS2 method is much less, which is consistent with the results in Example 5.1.

## Ternary collisions

We study ternary collisions by solving the NLD model (1.2) with the following initial data

$$\Psi(x,0)=\Psi_l^{ss}(x-x_l,0)+\Psi_m^{ss}(x-x_m,0)+\Psi_r^{ss}(x-x_r,0). \tag{5.8}$$

From Fig. 8 (obtained by the EPW method), we notice that the collision is almost elastic. After collision, the amplitudes of the left-traveling wave and the right-traveling wave become larger while the middle one becomes smaller.

Since the errors in discrete charge in this example are similar with those before, which are almost within the roundoff error of computer, we omit the results in this case. From the corresponding errors in Fig. 9, we can conclude that the energy and momentum are also preserved perfectly in this case. In detail, the present EPW and MSW methods conserve the energy conservation law a little better than MSWS1 and MSWS2 methods, meanwhile, MSWS1 and MSWS2 methods are more efficient in computations.

## 6 Conclusions

In this paper, based on wavelet collocation method in spatial discretization, we construct several structure-preserving algorithms for solving the nonlinear Dirac model. Firstly, we propose the EPW and MSW methods and investigate their conservative properties. We

https://doi.org/10.4208/aamm.2016.m1463 Published online by Cambridge University Press

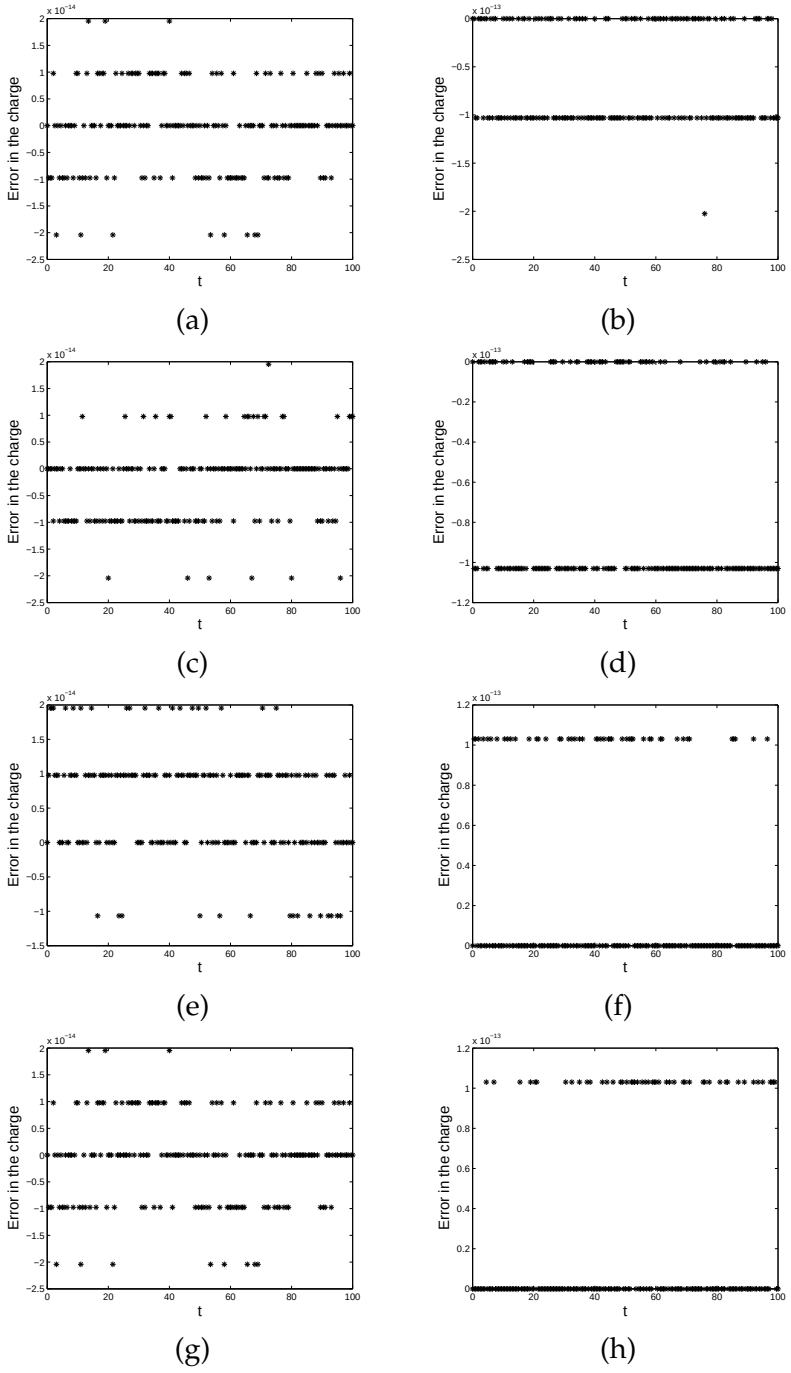



Figure 6: The errors in discrete charge with $\Lambda = 0.5$ (left) and $\Lambda = 0.2$ (right): (a), (b) EPW; (c), (d) MSW; (e), (f) MSWS1; (g), (h) MSWS2.

https://doi.org/10.4208/aamm.2016.m1463 Published online by Cambridge University Press

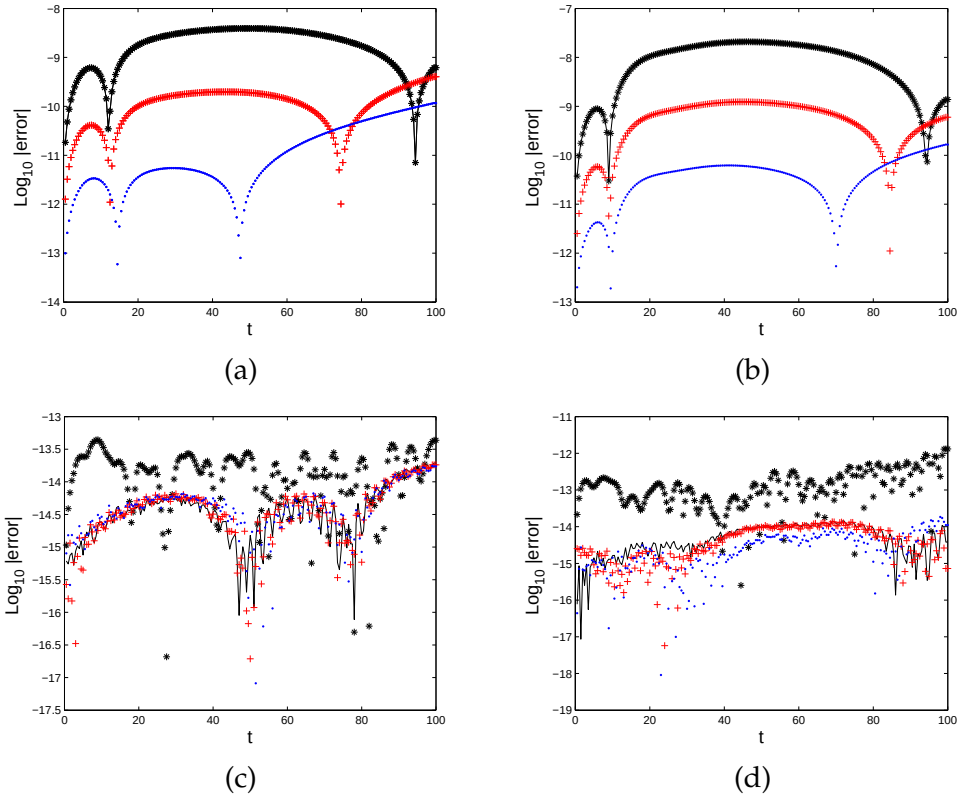



Figure 7: The errors in discrete energy (top) and momentum (bottom): $\Lambda=0.5$ (left); $\Lambda=0.2$ (right). Blue $\cdot$ symbols: EPW; Red $+$ symbols: MSW; Solid line: MSWS1; $*$ symbols: MSWS2.

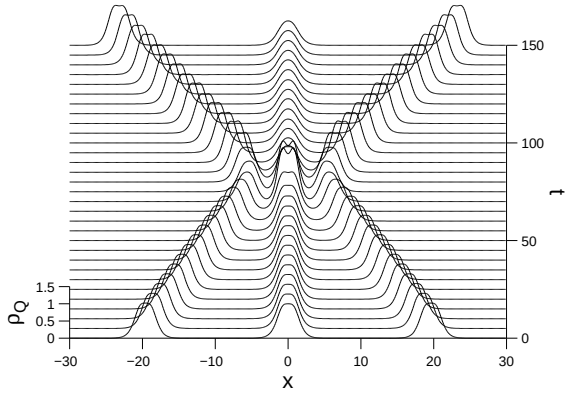



Figure 8: The collision of three solitons of the NLD model (1.2) by EPW with $v_l=-v_r=0.2$, $v_m=0$, and $x_r=-x_l=10$, $x_m=0$, $[x_L,x_R]=[-30,30]$.

https://doi.org/10.4208/aamm.2016.m1463 Published online by Cambridge University Press

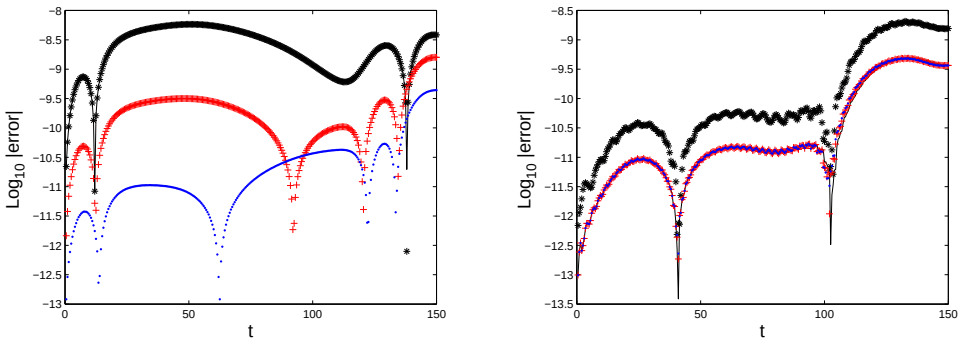



Figure 9: The errors in discrete energy (a) and momentum (b). Blue · symbols: EPW; Red + symbols: MSW; Solid line: MSWS1; ∗ symbols: MSWS2.

prove that both of them can preserve charge exactly. Meanwhile, the EPW method can preserve energy conservation law under appropriate conditions, and the MSW method can hold corresponding multi-symplectic geometric structure. To reduce the complexity and improve the efficiency in computations, we split the NLD equation into one linear subsystem and one nonlinear subsystem, and solve them separately. Furthermore, we take symplectic Euler integrator into the original scheme and achieve an efficient semi-explicit algorithm. Numerical experiments for solitary wave propagation and collision reveal that the proposed algorithms are stable and have corresponding structure-preserving properties in long-time simulations. Each of the four algorithms can preserve charge exactly. In particular, the EPW method performs best in terms of the accuracy and energy-preservation. Due to the reduction of computational complexity, the MSWS1 and MSWS2 methods need much less computational cost than the former EPW and MSW methods. Numerical results show the proposed algorithms are effective for the NLD equation and would be powerful mathematical tools for solving many other PDEs in mathematical physics.

## Acknowledgments

This work was supported by the National Natural Science Foundation of China (Grant Nos. 11501570, 91530106 and 11571366), Research Fund of NUDT (Grant No. JC15-02-02) and the fund from HPCL.

## References

[1] J. HONG AND C. LI, *Multi-symplectic Runge-Kutta methods for nonlinear Dirac equations*, J. Comput. Phys., 211 (2006), pp. 448–472.

https://doi.org/10.4208/aamm.2016.m1463 Published online by Cambridge University Press

[2] J. Xu, S. Shao and H. Tang, *Numerical methods for nonlinear Dirac equation,* J. Comput. Phys., 245 (2013), pp. 131–149.
[3] A. Alvarez, *Linear Crank-Nicholsen scheme for nonlinear Dirac equations,* J. Comput. Phys., 99 (1992), pp. 348–350.
[4] A. Alvarez and B. Carreras, *Interaction dynamics for the solitary waves of a nonlinear Dirac model,* Phys. Lett. A, 86 (1981), pp. 327–332.
[5] H. Wang and H. Z. Tang, *An efficient adaptive mesh redistribution method for a nonlinear Dirac equation,* J. Comput. Phys., 222 (2007), pp. 176–193.
[6] J. de Frutos and J. M. Sanz-Serna, *Split-step spectral schemes for nonlinear Dirac systems,* J. Comput. Phys., 83 (1989), pp. 407–423.
[7] S. Shao and H. Tang, *Interaction for the solitary waves of a nonlinear Dirac model,* Phys. Lett. A, 345 (2005), pp. 119–128.
[8] S. Shao and H. Tang, *Interaction of solitary waves with a phase shift in a nonlinear Dirac model,* Commun. Comput. Phys., 3 (2008), pp. 950–967.
[9] T. Bridges and S. Reich, *Multi-symplectic integrators: numerical schemes for Hamiltonian PDEs that conserve symplecticity,* Phys. Lett. A, 284 (2001), pp. 184–193.
[10] H. Zhu, L. Tang, S. Song, Y. Tang and D. Wang, *Symplectic wavelet collocation method for Hamiltonian wave equations,* J. Comput. Phys., 229 (2010), pp. 2550–2572.
[11] H. Zhu, S. Song and Y. Chen, *Multi-symplectic wavelet collocation method for Maxwell's equations,* Adv. Appl. Math. Mech., 3 (2011), pp. 663–688.
[12] H. Zhu, S. Song and Y. Tang, *Multi-symplectic wavelet collocation method for the nonlinear Schrödinger equation and the Camassa–Holm equation*, Comput. Phys. Commun., 182 (2011), pp. 616–627.
[13] X. Qian, Y. Chen and S. Song, *Novel conservative methods for Schrödinger equations with variable coefficients over long time,* Commun. Comput. Phys., 15 (2014), pp. 692–711.
[14] R. McLachlan and G. Quispel, *Splitting methods,* Acta Numer., 11 (2002), pp. 341–434.
[15] B. Ryland, R. Mclachlan and J. Frank, *On the multisymplecticity of partitioned Runge–Kutta and splitting methods,* Int. J. Comput. Math., 84 (2007), pp. 847–869.
[16] L. Kong, J. Hong, F. Fu and J. Chen, *Symplectic structure-preserving integrators for the two-dimensional Gross–Pitaevskii equation for BEC,* J. Comput. Appl. Math., 235 (2011), pp. 4937–4948.
[17] Y. Ma, L. Kong, J. Hong and Y. Cao, *High-order compact splitting multisymplectic method for the coupled nonlinear Schrödinger equations,* Comput. Math. Appl., 61 (2011), pp. 319–333.
[18] Y. Chen, H. Zhu and S. Song, *Multi-symplectic splitting method for two-dimensional nonlinear Schrödinger equation,* Commun. Theor. Phys., 56 (2011), pp. 617–622.
[19] X. Qian, S. Song and Y. Chen, *A semi-explicit multi-symplectic splitting scheme for 3-coupled nonlinear Schrödinger equation*, Comput. Phys. Commun., 185 (2014), pp. 1255–1264.
[20] X. Qian, S. Song, E. Gao and W. Li, *Explicit multi-symplectic method for the Zakharov–Kuznetsov equation,* China Phys. B, 21 (2012), 070206.
[21] S. Reich, *Multi-symplectic Runge-Kutta collocation methods for Hamiltonian wave equations,* J. Comput. Phys., 157 (2000), pp. 473–499.
[22] T. Bridges and S. Reich, *Multi-symplectic spectral discretizations for the Zakharov-Kuznetsov and shallow water equations,* Phys. D, 152 (2001), pp. 491–504.
[23] J. Chen and M. Qin, *Multi-symplectic Fourier pseudospectral method for the nonlinear Schrödinger equation,* Electron. Trans. Numer. Anal., 12 (2001), pp. 193–204.
[24] J. Chen, M. Qin and Y. Tang, *Symplectic and multi-symplectic methods for the nonlinear Schrödinger equation,* Comput. Math. Appl., 43 (2002), pp. 1095–1106.

https://doi.org/10.4208/aamm.2016.m1463 Published online by Cambridge University Press

[25] Y. WANG, J. JIANG AND W. CAI, *Numerical analysis of a multi-symplectic scheme for the time-domain Maxwell's equations,* J. Math. Phys., 52 (2011), 123701.
[26] A. AYDIN AND B. KARASÖZEN, *Symplectic and multi-symplectic methods for coupled nonlinear Schrödinger equations with periodic solutions,* Comput. Phys. Commun., 177 (2007), pp. 566–583.
[27] A. AYDIN AND B. KARASÖZEN, *Lobatto IIIA-IIIB discretization of the strongly coupled nonlinear Schrödinger equation,* J. Comput. Appl. Math., 235 (2011), pp. 4770–4779.
[28] J. FRANK, *Conservation of wave action under multisymplectic discretizations,* J. Phys. A Math. Gen., 39 (2006), pp. 5479–5493.
[29] J. FRANK, B. MOORE AND S. REICH, *Linear PDEs and numerical method that preserve a multi-symplectic conservation law,* SIAM J. Sci. Comput., 28 (2006), pp. 260–277.
[30] B. MOORE AND S. REICH, *Backward error analysis for multi-symplectic integration methods,* Numer. Math., 95 (2003), pp. 625–652.
[31] B. MOORE, *Conformal multi-symplectic integration methods for forced-damped semi-linear wave equations,* Math. Comput. Simul., 80 (2009), pp. 20–28.
[32] J. HONG AND Y. SUN, *Generating functions of multi-symplectic RK methods via DW Hamilton–Jacobi equations,* Numer. Math., 110 (2008), pp. 491–519.
[33] U. ASCHER AND R. MCLACHLAN, *Multisymplectic box schemes and the Korteweg-de Vries equation,* Appl. Numer. Math., 48 (2004), pp. 255–269.
[34] A. ISLAS AND C. SCHOBER, *On the preservation of phase space structure under multisymplectic discretization,* J. Comput. Phys., 197 (2004), pp. 585–609.
[35] Y. MIYATAKE, T. YAGUCHI AND T. MATSUO, *Numerical integration of the Ostrovsky equation based on its geometric structures,* J. Comput. Phys., 231 (2012), pp. 4542–4559.
[36] G. STRANG, *On the construction and comparison of difference scheme,* SIAM J. Numer. Anal., 5 (1968), pp. 506–517.

https://doi.org/10.4208/aamm.2016.m1463 Published online by Cambridge University Press